

# Research Journal of Pharmaceutical, Biological and Chemical Sciences

## Investigation of Mechanical Properties of Thermal Barrier Coating By Tested on a 4-point bending.

Ainar R. Ibragimov<sup>1</sup>, Tatiana A. Ilinkova<sup>2</sup>, Lenar N. Shafigullin<sup>1</sup>, Azat T. Gabdrakhmanov<sup>1</sup>, Rifat R. Sharipov<sup>2</sup>, and Aleksandr A. Lakhno<sup>3</sup>.

<sup>1</sup>Kazan Federal University, Russia, 423810, Naberezhnye Chelny, Prospect Mira, 68/19

<sup>2</sup>Kazan National Research Technical University named after A. N. Tupolev -KAI, Russia, 420111, Kazan, Karl Marks, 10

<sup>3</sup>Penza State Architecture and Construction University, Russia, 440028, Penza, Titov street, 28

### ABSTRACT

We have presented a new approach to determine the residual stress and energy characteristics of the deformation capacity of thermal barrier coating. This approach consist in obtaining deformation hysteresis that is determined in the deformation elastic zone in the four-point static bending. We have introduced a concept of estimation of relaxation energy density in the elastic zone of deformation of thermal barrier coating.

**Keywords:** Thermal barrier coating, 4-point bending test, elastic properties, high temperature test

*\*Corresponding author*

## INTRODUCTION

Usage of ceramic thermal barrier coatings (TBC) based on partially stabilized  $ZrO_2 - 6-8Y_2O_3$  zirconia oxide of 0.2 ... 1 mm thickness sprayed on the chamber parts surface, nozzle and rotor blades of the turbine engine is widely used in the manufacture of gas turbine engines.  $ZrO_2 - 6-8Y_2O_3$  coating have a low degree of blackness and a low thermal conductivity that reduces the surface temperature of the details to 373-443K depending on the coating thickness and the cooling intensity [1]. Thermal barrier coatings on the combustion chamber parts of the gas turbine engine are typically double-layered, under the external ceramic layer is applied heat resistant bond coat of Ni-Co-Cr-Al-Y protects the parts surface against high temperature oxidation and salt corrosion. Coating is carried out by plasma spraying.

During the coating formation, there are internal stresses in it; their level depends on the non-uniformity degree of the spraying powder particles sizes, penetration, availability of hard contact with metal substrate, differences of coefficients of thermal expansion and Young modulus for materials of both layers of coating and metal substrate [2, 3]. These factors together create a significant scattering of mechanical properties of the coating [4]. Therefore the basis of the recent research trends in the field of study of the mechanical properties of plasma multi-layer TBC lies in identifying patterns of their changes in connection with coating parameters [5].

Efficiency of thermal barrier coatings is determined by their thermal conductivity, thermal stability, and value residual stresses [6], and mechanical properties of adhesion and cohesion strength, the resistance of the thermo-mechanical fatigue [7]. According to safety and durability of the coatings their strength and deformation capacity is the most significant parameters.

Research method of the coatings strength and deformation properties under four-point bending is qualitatively different from the three-point method [8, 9]. This method allows to determine mechanical properties of "the coating - base metal" system of sufficiently large volume [10] which fully reflect the real properties of the system [11].

Behavioral analysis of thermal barrier coatings under static four-point bending shows that mechanical properties of coatings obtained during testing can be used to optimize the coating and "coating – substrate" system: implementing the selection of powder materials, determination of optimal thickness of two-layer coating, coating parameters [9,10]. However selection criteria may be such characteristics as stress cracking and coating breaking stress, elastic modulus (Young's modulus) of a ceramic thermal barrier layer, the rigidity of the "composite cover - substrate" system. At the same time, this method can be used successfully for studying the deformation properties of the coatings in the elastic-plastic area in case of usage highly sensitive means of measuring the force and displacement of the sample at the process of deformation.

## OBJECTS AND METHODS OF RESEARCH

Heat-resistant alloy VH-4A on the nickel basis (HN50VMTYUB, made in Russia) used for the manufacture of parts of the combustion chamber of the gas turbine engine [12, 13] and based on a review of studies of interaction with metal coatings [14,15] was selected as for the deposition of test samples of thermal barrier coatings.

Two types of nickel-based powders: PV-NH16Y6It and PNH20K20Y13 (made in Russia) were chosen as materials for bond coat.

The following two types of powders of zirconium oxide, 7-8% stabilized yttrium oxide were used for coating the external ceramic layer:

- CIO-7-10-50 by "TCP" company, Russia;
- Z7Y-10-90 by LLC " Research Institute TSPS - Saturn", Russia.

All of the powder have a spherical shape. Fractional composition of the powder is given in Table 1.

**Table 1 - Fractional composition of the powder for ceramic layer of TBC (%)**

| particle size, $\mu\text{m}$ / powder brand | CIO-7-10-50 | Z7Y-10-90 |
|---|-------------|-----------|
| +125  | -           | -         |
| +90   | -           | less >3   |
| +63   | -           | -         |
| +45   | -           | -         |
| +45-56                                      | 9,0         | -         |
| +40-90                                      | -           | less >7   |
| -45   | 89          | -         |
| +20-40                                      | -           | 80        |
| -20   | -           | 10        |

Chemical composition of powder of the TBC ceramic layer is differ by composition and content of the impurities (Table 2).

**Table 2 - Chemical composition of powder of the TBC ceramic layer (% wt)**

| Material brand | Chemical composition, % |                |                         |                         |                |
|----------------|-------------------------|----------------|-------------------------|-------------------------|----------------|
|                | $\text{Y}_2\text{O}_3$  | $\text{SiO}_2$ | $\text{Fe}_2\text{O}_3$ | $\text{Al}_2\text{O}_3$ | $\text{TiO}_2$ |
| CIO-7-10-50    | 7 $\pm$ 1               | 0,05           | 0,05                    | 0,2                     | less >0.1      |
| Z7Y-10-90*     | 7,5 $\pm$ 0,5           | 0,02           | 0,05                    | 0,05                    | 0,02           |

All powders base –  $\text{ZrO}_2$ . \*Additionally consist to 0,05 % MgO и CaO.

Before applying the bond coat, surface of slabs of VH-4A alloy was treated by abrasive-jet method with fine granulation corundum (0.8-1.0 mm). Operating air pressure for transporting of abrasive was about 0.3 ... 0.4 MPa. After the treatment, the thickness of slabs was measured with an accuracy to 1  $\mu\text{m}$  and a surface roughness was determined by profilometer. The average roughness  $R_a$  of the slab surface was 6 -12  $\mu\text{m}$ . After abrading slabs were blown by argon to remove residual abrasive particles.

Bond coats of powder materials PNH20K20Y13, PV-NH16Y6 were applied according to order set forth in the Table 2, on the one side of the slab. After applying the bond coat roughness  $R_a$  was 6-9  $\mu\text{m}$ .

Ceramic layers of different thicknesses of the powder materials Z7Y-10-90, CIO-10-07-50 were covered on a robotic plasma generator UPU-8M for 5 passes according to order set forth in the Table 3.

**Table 3 - Technological parameters of TBC depositing on the plasma generator UPU-8M**

| Coating mode                                   | bond coat   | ceramic     |
|--|-------------|-------------|
| Coating distance, mm                           | 100-105     | 100-105     |
| Current rate, A                                | 380-400     | 420-450     |
| Voltage, V                                     | 60-65       | 65-68       |
| Consumption Ar, l/ min (plasma-supporting gas) | 50-55       | 40-45       |
| Hydrogen pressure, $\text{kgf}/\text{cm}^2$    | 3 $\pm$ 0,2 | 3 $\pm$ 0,2 |
| Consumption Ar, l/ min (lift gas)              | 3-4         | 4-5         |
| Argon pressure, $\text{kgf}/\text{cm}^2$       | 5 $\pm$ 0,2 | 5 $\pm$ 0,2 |
| Coating speed, mm/s                            | 85          | 50          |
| Powder consumption, $\text{kg}/\text{h}$       | 1-1.3       | 1.2-1.5     |
| Passing width, mm                              | 5,0         | 5,0         |

Slabs during deposition of ceramics were forcibly cooled to 350–400  $^{\circ}\text{C}$  with air.

After deposition, the coated slabs were put to a double heat treatment according the regime:

- Diffusion annealing in vacuum at a temperature 1050°C for 4 hours to restore the bulk properties of the substrate material.
- Oxidation annealing in the air at 850°C within 20 hours. Oxidative annealing restores the stoichiometry of zirconium oxide, and provides the necessary completeness of diffusion processes in the “coverage – substrate” area.

After deposition the samples were thermally treated by two ways: 1) vacuum diffusion annealing at 1050°C for 4 hours; 2) vacuum diffusion annealing 1050°C for 4 hours + oxidation annealing at 850°C for 2 hours.

The thickness of the ceramic layer is ranged from 230 μm to 780 μm, the bond coat is from 50 μm to 200 μm. Thickness was determined on microsections on the universal metallographic microscope Axiovert 200 MAT using the AxioVision program.

After that, slabs with coating for investigating the mechanical properties were cut by electrospark discharge machine to samples with size of 10×80×2 mm. As long as ceramic layer of the coating does not conduct electric current, it was cut with a diamond disk.

Strain indicator of 2PKB type were glued to measure the deformation of individual layers of the system on substrate surface and coating. Prepared test samples were loaded by four point bending scheme at room temperature so that the coating between the supports was subjected to tensile loads.

As a loading device we used a FPZ 100/1 tensile machine, ensuring smooth loading with a minimum speed (0.02 ... 0.84 mm / min), small loads, not more than 10 kN, and measuring deformations of small dimensions.

Scheme of loading and general view of the device with the sample installed on the machine are shown in Figure 1.

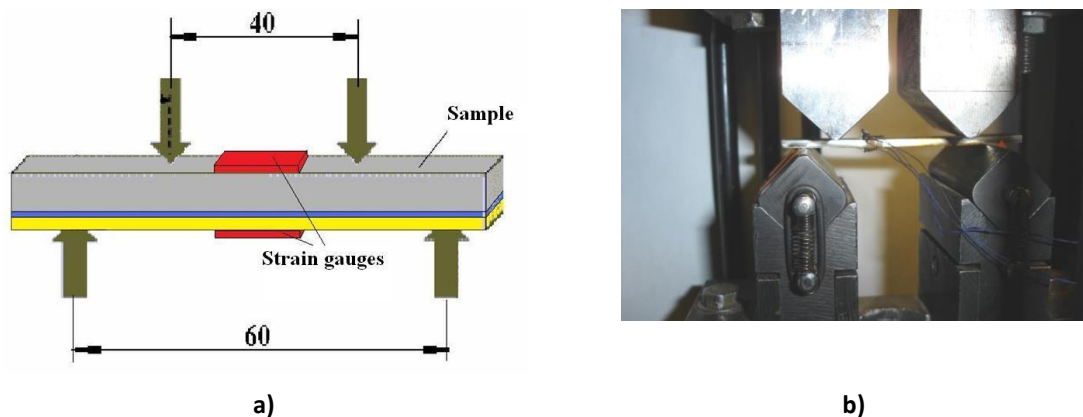


**Figure 1: Scheme of loading and general view of the device: a) loading scheme; b) overall view of the attachment**

To measure the forces and deformations we used automatic Program Apparatus Complex ACTest, providing strain measurement of small size. Strain module connected with strain gauges on the one hand, and the data acquisition device for deformation information of type LTR212, on the other.

Module of analog digital converter is connected to the FPZ 1/100 tensile machine, on the one side, and to the LTR11 data acquisition device on the other. Both data acquisition devices are connected in 2-seater portable crate LTR that has an interface USB 2.0, which is connected to the computer and operated on software. All the LTR modules have passed verification for the accuracy of measurement.

### EXPERIMENTAL RESULTS AND DISCUSSION

The study purpose was to obtain deformation curves during loading and unloading in the elastic-plastic area. Experimentally matched load of 400 N was chosen as the maximum.

Analysis of typical deformation curves of the ceramic coating layer of CIO-7-10-50 (Fig.2a) and Z7Y-10-90 brands (Fig.2b) shows the presence of the deformation hysteresis. This goes to prove the inelastic way of deformation of coatings at low load, which is shown in the delay of elastic deformation development under the influence of an external load. Hysteresis is shown in the misalignment of crossed lines of deformation for loading and unloading, as an obvious consequence of laws of plastic deformation.

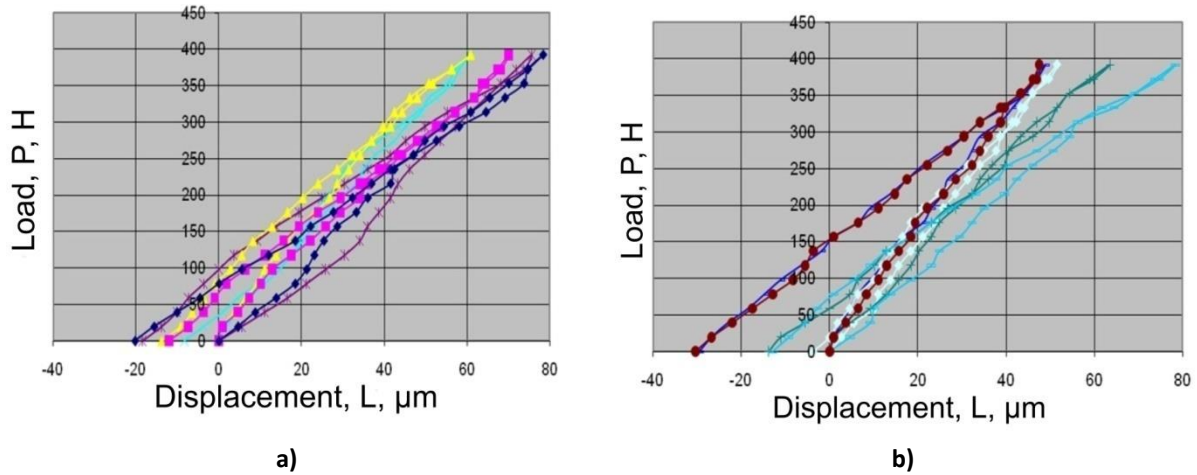


**Figure 2: Strain curves of the ceramic coating layer brands CIO-07-10-50 (a) and Z7Y-10-90 (b)**

The phenomenon of inelasticity in different materials had been studied by A.S.Novik [16], K.Ziner, Ke Ting-sui [17], they concluded that inelasticity occurs only in visco-elastic materials and depends on the rate of load application. The higher the rate, the bigger will be the hysteresis loop. With a very low voltage application rate, equivalent to its relaxation, area size of the loop may be equal to zero. So in our experiment deformation rate was calculated by fractions of a millimeter per minute, and the deformation hysteresis was obtained in all cases, we assume that the studied systems are visco-elastic media.

The deformation lag behind the stress may be caused by different kinds of imperfections of coating structure, especially viscous medium in elastic coating material - porosity, interlayer surfaces and grain boundaries, their viscous nature of deformation has been proven by Ke Ting-sui [17].

Causes of inelasticity create internal friction in the material. Apparently, the main mechanism of deformation of plasma TBC depends on the volume and pores distribution, micro-cracks, and the glassy phase.

Under these loading conditions, deformation hysteresis had the form of a fundamentally different type in contrast to the hysteresis of elastic-plastic nature. Thus, during descent the external tensile stress applied to the coating, load curve gradually moved up higher the loading curve. After the complete removal of deformation in the coating regardless of its type, there is always residual stress (Fig. 2a and 2.b).

This fact could be explained by following.

When the load is on the maximum value, the elastic and viscous coverage zones get a homogeneous deformation. Immediately after that, stress relaxation process starts in the viscous zone. It is reverse realignment that captures boundary areas of the elastic zone. During descent of the load, here occurs the elastic deformation of the opposite sign, i.e. voltage will decrease and gradually disappear far from the boundaries in the elastic zone, but on the borders stress state is still exist, and its concentration in local areas can be significant. Residual stresses developed in the unstable process of deposition are added to stress state; the result is expressed in a shift of the unloading curve in the position above the loading curve. To completely remove the stress state in the coating it is necessary to apply compressive deformation to the sample. Adjusting the stress to zero, we will get the value of the residual compressive deformation. Energy dissipation at a very low rate of deformation is taken away.

Since the work absorbed during deformation is characterized by area under the corresponding diagram, it is obvious that the area of hysteresis loop or the difference between the absorbed work during loading and returned work during unloading reflects the residual deformation work, which is not returned during unloading.

Analysis of deformation curves showed that absolute compression set in the investigated coatings with few exceptions are approximately equal and reach to  $-15 \mu\text{m}$ , which indicates about comparable conditions of coating formation during deposition. Comparing the values of residual deformation with coating thickness, it is arguable that there is no strict connection between these characteristics. Comparable values of residual deformations for coatings of both high and low values were obtained.

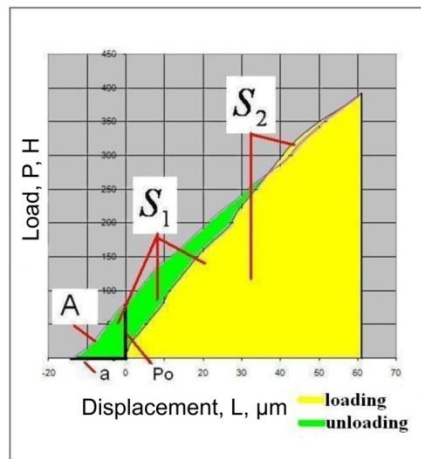


**Figure 3: Stress-strain diagram of the ceramic coating layer in the process of loading and unloading**

However more significant differences in the behavior of studied TBC systems could be obtained by determining the energy (work) expended for releasing of internal stresses, requiring deformation of the system in the compression area. This energy was determined by the area under the unloading curve, and its part (the area A in Fig. 3) in the compression area. The difference of the areas under the loading curve  $S_1$  and unloading curve  $S_2$  provides the work (energy) required to release internal stresses:

$$S = S_1 - S_2 \tag{1};$$

where  $S_1$  is the area under the loading curve, J;  $S_2$  is the area under the unloading curve, J. The calculation of these areas can be done by formulas (2), (3):

$$S_1 = \sum_{i=1}^n |L_i| \cdot P_{n1} \tag{2};$$

$$S_2 = \sum_{i=1}^n L_i \cdot P_{n2} \tag{3};$$

where  $P_{n1}$  is loading, N;  $P_{n2}$  is unloading, N;  $L_i$  is a movement,  $\mu\text{m}$ .

The value of  $S$  always takes a negative value, which means that after unloading of the coating more energy is released compared to the process of loading of the coating. This difference is the value of internal energy that is released during unloading. It allows to characterize the stress state of coatings formed during the deposition process. We can calculate the work  $A$  expended for the full release of the internal stresses in the coating in compression area, as an area of a right triangle:

$$A = \vec{P} \cdot \vec{a} = F \cdot a \cdot \cos \varphi = \left( a \cdot \sqrt{a^2 + P_o^2} \right) \cos \varphi \tag{4};$$

where: A is work for release of internal stresses in the compression coatings, J.; P is force, N;  $a$  is a movement in compression area,  $\mu\text{m}$ ,  $P_0$  is a residual force, N.

Residual stresses  $\sigma_{r.s.}$  released in the coating are calculated according to the formula:

$$\sigma_{r.s.} = \frac{3P_0 \cdot C}{B \cdot H^2}, \text{ MPa} \quad (5);$$

where  $P_0$  is the residual stress wherein the deformation becomes zero; B is width of the sample, mm; H is the total thickness of the sample, mm; C is the distance between loaded and support beam, 10 mm.

*The energy density of the elastic deformation.* The total energy of elastic deformation U, J., occurring under tension in the solid material is calculated by the simplified formula [18]:

$$U = \frac{P_m L}{2}, \quad (6);$$

where  $P_m$  is a maximum force, MPa; L is displacement (total deformation),  $\mu\text{m}$ . Equation can be converted for prismatic bar (6) using Hooke's law to the following form:

$$U = \frac{P_m^2 L}{2FE} \quad (7);$$

$$\text{or } U = \frac{FEL^2}{2L} \quad (8);$$

The first of these equations allows to determine the energy of elastic deformation as a force function,  $P_m$ , and the second as a displacement function L. In practical applications, the important thing is the energy of elastic deformation, referred to unit volume, i.e. the energy density. According equations (6) and (7) it is:

$$U' = \frac{U}{FL} = \frac{\sigma_{r.s.}^2}{2E} \quad (9);$$

where  $\sigma_{r.s.} = P_m / F$  is tensile stress.

The elasticity modulus E of three-layered system (substrate – bond coat - ceramic layer) using additivity rule, is calculated by:

$$E = \frac{E_{sub.} h_{sub.} + E_{b.c.} h_{b.c.} + E_{t.c.} h_{t.c.}}{H} \quad (10);$$

where:  $E_{sub.}$ ,  $E_{b.c.}$ ,  $E_{t.c.}$ , are modules of the base elasticity, the bond layer and a ceramic layer, respectively, GPa;  $h_{sub.}$ ,  $h_{b.c.}$ ,  $h_{t.c.}$  – thickness of the base, the bond layer and a ceramic layer,  $\mu\text{m}$ .

The elasticity modulus of the bond coat and the ceramic layer was determined according to the authors methods [8,9].

Using equation (10), let's calculate the density of elastic energy  $U'_0$ , released in the compression area, using the formula (5):

$$U'_0 = \frac{\sigma_{r.s.}^2}{2E} = \frac{\left(\frac{3P_0 \cdot C}{B \cdot H^2}\right)^2}{2\left(\frac{E_{sub.} \cdot h_{sub.} + E_{b.c.} \cdot h_{b.c.} + E_{t.c.} \cdot h_{t.c.}}{H}\right)} \quad (11);$$

As long as thermal barrier coatings are operated at high temperatures for a long time, in both of the coating layers irreversible changes are in process that lead not only to sealing the porous and fractured system, but also to the complete disappearance of micro-cracks and pores. Coating becomes dense, the thermal insulation degree and its resistance decreases. Therefore it is important to know how elastic properties of the coating could change after the high temperature operating time.

**Table 4 - The elastic characteristics of thermal barrier coatings before and after high-temperature exposure**

| No. of sample      | $h_{t.c.}$ ,<br>μm | $h_{t.c.}/$<br>$h_{b.c.}$ | $L_m$ ,<br>(μm<br>) | $P_0$ ,<br>H | $a$ ,<br>μm | $A \cdot 10^{-6}$ , J | $S$<br>$\cdot 10^{-6}$ , J | $\sigma$ ,<br>MPa | $U'_0$<br>$\cdot 10^{-19}$ ,<br>J/m <sup>3</sup> | $E_{t.c.}$<br>$\cdot 10^3$ , MPa |
|--------------------|--------------------|---------------------------|---------------------|--------------|-------------|-----------------------|----------------------------|-------------------|--|----------------------------------|
| 1                  | 2                  | 3                         | 4                   | 5            | 6           | 7                     | 8                          | 9                 | 10   | 11                               |
| <b>CIO-7-10-50</b> |                    |                           |                     |              |             |                       |                            |                   |  |                                  |
| 1-1                | 300                | 3,0                       | 61                  | 83,3         | -14         | -532,9                | -1917                      | 43,4              | 5,38   | 35,3                             |
| <b>100h.</b>       |                    |                           |                     |              |             |                       |                            |                   |  |                                  |
| 2-1                | 360                | 1,9                       | 61                  | 35,3         | -8          | -153,5                | -941                       | 16,3              | 0,78   | 22,0                             |
| 2-2                | 360                | 1,9                       | 42                  | 70,6         | -15         | -313                  | -372                       | 32,6              | 3,13   | 21,7                             |
| <b>50h.</b>        |                    |                           |                     |              |             |                       |                            |                   |  |                                  |
| 11-2               | 417                | 3,1                       | 110                 | 16,3         | -5          | 25,3                  | 1951                       | 7,5               | 0,17   | 14,5                             |
| <b>10h.</b>        |                    |                           |                     |              |             |                       |                            |                   |  |                                  |
| 3-1                | 470                | 2,5                       | 76                  | 98,0         | -18         | -867,1                | -5798                      | 41,9              | 5,39   | 10,9                             |
| 3-2                | 470                | 2,5                       | 61                  | 19,6         | -3          | -27.6                 | 1002                       | 8,4               | 0,22   | 11                               |
| <b>2h.</b>         |                    |                           |                     |              |             |                       |                            |                   |  |                                  |
| 4-1                | 545                | 4,5                       | 70                  | 65,3         | -12         | -352,3                | -1545                      | 27,5              | 2,43   | 7,4                              |
| 4-2                | 545                | 4,5                       | 73                  | 65,3         | -4          | -114,6                | 1271                       | 21,45             | 2,43   | 7,4                              |
| <b>1 h.</b>        |                    |                           |                     |              |             |                       |                            |                   |  |                                  |
| 5-1                | 670                | 5,3                       | 78                  | 78,4         | -20         | -794,8                | -2290                      | 30,0              | 3,04   | 4,4                              |
| 5-2                | 670                | 5,3                       | 70                  | 0            | 0           | 0                     | 2214                       | 0                 | 0  | 4,4                              |
| <b>Z7Y-10-90</b>   |                    |                           |                     |              |             |                       |                            |                   |  |                                  |
| 6-1                | 270                | 3,4                       | 49                  | 150,3        | -29         | -2294,2               | -5134                      | 81,6              | 18,72  | 47,1                             |
| <b>100h</b>        |                    |                           |                     |              |             |                       |                            |                   |  |                                  |
| 7-1                | 300                | 4,1                       | 52                  | 19,6         | -4          | -36,1                 | -1214                      | 10,5              | 0,31   | 36,2                             |
| 7-2                | 300                | 4,1                       | 48                  | 45,7         | -5          | -115                  | 509                        | 14                | 1,69   | 36                               |
| <b>50h</b>         |                    |                           |                     |              |             |                       |                            |                   |  |                                  |
| 8-1                | 325                | 2,0                       | 64                  | 58,8         | -14         | -460,6                | -1718                      | 28,5              | 2,35   | 29,0                             |
| 8-2                | 325                | 2,0                       | 57                  | 39,2         | -5          | -92                   | 1643                       | 9,5               | 1,04   | 28,4                             |
| 1                  | 2                  | 3                         | 4                   | 5            | 6           | 7                     | 8                          | 9                 | 10   | 11                               |
| <b>10h</b>         |                    |                           |                     |              |             |                       |                            |                   |  |                                  |
| 9-1                | 415                | 6,2                       | 78                  | 73,5         | -13         | -469,7                | -2850                      | 35,9              | 3,88   | 14,9                             |
| 9-2                | 415                | 6,2                       | 60                  | 4,9          | -1          | -9,2                  | 1274                       | 2,4               | 0,02   | 15,3                             |
| <b>2h</b>          |                    |                           |                     |              |             |                       |                            |                   |  |                                  |
| 10-1               | 775                | 6,7                       | 47                  | 152,9        | -30         | -2194,8               | -4961                      | 54,9              | 10,51  | 3,1                              |
| 10-2               | 775                | 6,7                       | 53                  | 16,8         | -3          | -27.6                 | 420                        | 6                 | 0,13   | 3,1                              |

The second half of the samples (index 2 in the specimen designation) of TBC investigated systems was kept in the oven at a temperature of 1373K with variation of exposure time from 1 to 100 hours depending on the ceramic coating layer thickness. The testing time of each sample was reduced in accordance with decrease of thickness of the ceramic layer to prevent destruction of the coating. Samples with a operating time more



than 10 hours actually were kept on the treatment of "isothermal holding", its cycle frequency was 7 hours. Cooling of the samples was carried out with the oven. After high-temperature exposure, the samples were tested under conditions similar to those described above. The results of the measurements are presented in the table 4.

Let's consider the calculation results of elastic characteristics of the studied thermal barrier coatings before high temperature exposure process. With increasing of ceramic layer thickness in both coating compositions Young's modulus reduces, which is obviously related to accumulation of structural discontinuities: microcracks, volume porosity, and also increasing the total area of interlayer surfaces. Therefore, Young's modulus for such discrete media can be considered structurally dependent characteristic which varies depending on the deposition method and conditions, powders morphology, and the coating formation conditions.

The value of residual stresses in coatings on average is about 28 MPa (for CIO-07-10-50) and 42 MPa (for Z7Y-10-90) and in general does not depend on the coating thickness: high residual stresses obtained for coating with a minimum thickness of 270-300  $\mu\text{m}$  and they are low enough for coatings with a thickness exceeding 500  $\mu\text{m}$ . Obviously, instability modes of plasma coating, the heterogeneity of the particle grain size leads to a significant dispersion of the residual stresses value.

The density of elastic energy at the compression area of deformation hysteresis more fully reflects the system state because it takes into account the value of Young's modulus of the ceramic layer, its thickness and value of the residual stresses remaining in the complete unloading of sample.

Long term exposure at high temperature of thermal barrier coatings significantly changes its elastic characteristics and residual stresses level in the coating after deposition, and double heat treatment. So one hour during exposure in the CIO-07-10-50 coating there was complete relaxation of internal stresses. However, the value of Young's modulus was not changed.

Energy  $A$  (from 3 to 80 times), energy density  $U'_0$  for Z7Y-10-90 coating were reduced to 80 times in both coatings within 2 hours of exposure. Energy  $S$  has changed quite significantly: residual plastic deformation appeared in the coating. Perhaps they were due to high-temperature creep of metallic substrate, which arises due to CTE difference of three components: ceramic, bond coat and the substrate. Because of the higher adhesion forces occurring in the process of coating formation, the total plastic strain relaxation (shrinkage) during bond coat cooling can not be possible.

The increase of exposure time to 10-50 hours contributes to continuing reduction of residual stresses, elastic energy and its density but to a smaller degree by far. Increasing processes of sintering of ceramic layer is an opposing force, which prevents reduction of coating stress state.

100 hours of isothermal exposure is a crash time when sintering forces overcome the relaxation force of internal stresses. In both types of coatings increase of residual stresses (from 1.4 to 2 times) and all energy characteristics ( $A$ ,  $S$ ,  $U'_0$ ) are observed.

In this case, significant changes in the Young's modulus value almost did not happen.

## CONCLUSION

Thus, the obtained results allow to confirm that the proposed energy elastic characteristics of thermal barrier coatings:  $S$ ,  $A$ ,  $U'_0$  are significantly more sensitive to the kinetics of sintering processes that occur during high-temperature exposure than Young's modulus. These characteristics allow to distinguish little differences in the behavior of thermal barrier coatings systems of different composition and thickness, which is very important to create a reliable high-efficiency coatings.

Analysis of change of energy elastic properties in CIO-7-10-50 and Z7Y-10-90 coatings with increasing time of isothermal exposure has shown that the most intensive decrease of these characteristics occurs in the first 1-2 hours. After that the reduction degree falls, and starting with 100th hour of isothermal exposure, stress state of the system begins to increase and the elastic energy starts to accumulate.

## REFERENCES

- [1] Inozemtsev A.A., Sandratsky V.L. Gazoturbinyi dvigateli [Gas turbine engines]. Perm, Aviodvigatel, 2006, 1204 p.
- [2] Mitina B.S. Poroshkovoi metallurgiya i napilenie pokritia [Powder metallurgy and sprayed coatings]. Metallurgy, Moscow, 1987, 791 p.
- [3] Taylor R., Brandon J.R., Morrel P. Microstructure, Composition and Property Relationships of Plasma-Sprayed Thermal Barrier Coatings. *Surface and Coatings Technology*, 1992, 50, pp. 141 – 149
- [4] Clyne T.W., Gill S.C. Residual Stresses in Thermal Spray Coatings and their Effect on Interfacial Adhesion: a Review of Recent Work, *Journal Thermal Spray Technology*, 1996, 5, pp. 401 - 418
- [5] Kucuk A., Berndt C.C., Senturk U. et al. Influence of plasma spray parameters on mechanical properties of yttria stabilized zirconia coatings. I: Four point bend test, *Materials Science and Engineering*, 2000, A284, pp. 29 - 40
- [6] Matejicek J., Sampath S., Dubsy J., *Journal of Thermal Spray Technology*, 1998, 7, pp. 489 - 496
- [7] Senturk U., Lima R.S., Berndt C.C. et al., Processing and Mechanical Properties of Plasma Sprayed Thermal Barrier Coatings, in *Proceeding of United Thermal Spray Conference*, E. Lunscheider and P.A. Kammer (Ed.), German Welding Society (Dusseldorf, Germany), 1999, pp. 815 - 819
- [8] Beghini M., Bertini L., Frenzo F., Measurement of Coatings' Elastic Properties by Mechanical Methods: Part 1. Consideration on Experimental Errors, *Experimental Mechanics*, 2001, 4 (41), pp. 293 - 304
- [9] M. Beghini, G. Benamati, L. Bertini, F. Frenzo, Measurement of Coatings' Elastic Properties by Mechanical Methods: Part 2. Application to Thermal Barrier Coatings, *Experimental Mechanics*, 2001, 41, No. 4, p 305-311
- [10] Berndt C.C., Kucuk A., Dambra C.G., Influence of plasma spray parameters on behavior of yttrium stabilized zirconium the cracking coatings, *Practical failure analysis*, 2001, I, pp. 55 - 64
- [11] ASTM C158-02 (2007) Standard test methods for strength of glass by flexure (Determination of Modulus of Rupture), *Electronical resource*, ASTM. URL: [www.astm.org/Standards/C158.htm](http://www.astm.org/Standards/C158.htm)
- [12] Kuznetsov V.P., Lesnikov V.P., Khadyev M.S., Konakova I.P., Popov N.A. Structural and phase transformations in single- crystal alloy ZHS36-VI [001] after holding in the range of 1050-1300°C, *Metal Science and Heat Treatment*, 2012, 1(54), pp. 90-95
- [13] Terent'ev D.S., Shevtsova L.I., Mali V.I., Bataev A.A., Bataev I.A., Lozhkin V.S. Structure and properties of composite materials «aluminum- nicel aluminide» produced by the SPS method, *The 8 International Forum on Strategic Technology, IFOST 2013 proseedng*, 2013, pp. 187 - 189.
- [14] Budovskikh E.A., Gromov V.E., Romanov D.A. The Formation Mechanism Providing High-Adhesion Properties of an Electric-Explosive Coating on a Metal Basis, *Doklady Physics*, 2013, 3 (58), pp. 82 – 84.
- [15] Xia G., Chen Z., Saifutdinov A.I., Eliseev S., Hu, Y., Kudryavtsev A.A. Longer Microwave Plasma Jet With Different Discharge Performances Originated by Plasma Surface Interactions, *IEEE Transactions on Plasma Science*, 2014, 10 (42), pp. 2768 – 2769.
- [16] Postnikov V.S. *Vnutrynee trenyi v metallax [The success of Metal Physics]*. Moscow, Metallurgy, 1974, 352 p.
- [17] Ting- Sui Ke, Zener C., Determination of metal structures , past the cold treatment by measuring the inelastic phenomena collection [Determining the structure of metals , past the cold treatment by measuring the inelastic phenomena], Moscow, Foreign Literature Publishing House, 1954, pp. 21 – 23.
- [18] Timoshenko S.P. *Soprotivliniy materialov [Timoshenko Strength of Materials]*, Moscow, Nauka, 1965, pp. 255 – 257.